Thermally induced rotation of 3*d* orbital stripes in $Pr(Sr_{0.1}Ca_{0.9})_2Mn_2O_7$

T. A. W. Beale,[1] S. R. Bland,[1] R. D. Johnson,[1] P. D. Hatton,[1,*] J. C. Cezar,[2] S. S. Dhesi,[3] M. v. Zimmermann,[4] D. Prabhakaran,[5] and A. T. Boothroyd[5]

[1]*Department of Physics, University of Durham, Rochester Building, South Road, Durham DH1 3LE, United Kingdom*

[2]*European Synchrotron Radiation Facility, Boîte Postal 220, F-38043 Grenoble Cedex, France*

[3]*Diamond Light Source Ltd, Harwell Science and Innovation Campus, Diamond House, Chilton, Didcot, Oxfordshire OX11 0DE, United Kingdom*

[4]*Hamburger Synchrotronstrahlungslabor (HASYLAB), Deutsches Elektronensynchrotron (DESY), 22605 Hamburg, Germany*

[5]*Department of Physics, University of Oxford, Clarendon Laboratory, Parks Road, Oxford OX1 3PU, United Kingdom*

(Received 13 January 2009; revised manuscript received 4 February 2009; published 27 February 2009)

We have investigated orbital ordering in the bilayer manganite, $Pr(Sr_{0.1}Ca_{0.9})_2Mn_2O_7$, using synchrotron x-ray diffraction techniques, in particular resonant soft x-ray diffraction. Diffraction signals are observed at $(0,\frac{1}{2},0)$ above 300 K and $(\frac{1}{2},0,0)$ below 300 K, corresponding to orbital stripes along the *a* and *b* axes, respectively. The previously observed transition at 300 K is evidence of a rotation of the orientation of the 3*d* orbital stripes. Large resonances of the orbital signals are observed at the Mn *L* edges, with a complex dependence on incident photon energy indicative of a weakly Jahn-Teller distorted system. A structural transition observed at 92 K is found not to involve a further change in the orbital order.

DOI: 10.1103/PhysRevB.79.054433 PACS number(s): 75.47.Lx, 75.50.Ee, 75.60.Ch, 78.70.Ck

I. INTRODUCTION

The application of the semicovalent exchange theory to the manganite series[1] initiated the drive to observe and understand the charge and orbital orderings and their complex interaction with magnetic order.[2–4] This research has advanced to the point where the control and exploitation of these order parameters is becoming possible, developing the field of spintronics and orbitronics.[5] For example, the mediation of the orbital state has been pioneered through applying stress to tetragonal $La_{1-x}(Sr,Ca)_xMnO_3$ thin films, coupling the Jahn-Teller distortions to the uniaxial strain.[6,7] This causes a preferential occupancy of the manganese 3*d* orbitals in a single direction.

In this paper we study the thermal switching of occupied orbitals in the bilayer manganite $Pr(Sr_{0.1}Ca_{0.9})_2Mn_2O_7$ (Fig. 1) by soft x-ray diffraction at the Mn $L_{2,3}$ edges. This technique is directly sensitive to Mn 3*d* electron orbitals through the resonant enhancement of the $2p \rightarrow 3d$ dipole transition. Unlike many manganites, $Pr(Sr_{0.1}Ca_{0.9})_2Mn_2O_7$ crystallizes into the orthorhombic space group, *Amam*, with lattice parameters $a=5.410$ Å, $b=5.462$ Å, and $c=19.277$ Å at 405 K. This *Amam* space group is a hettotype of the higher symmetry tetragonal $I4/mmm$, and is required as a consequence of the tilting of the MnO_6 octahedra. The orthorhombic lattice, above the orbital order transition, has been shown to confine the formation of the orbital order to a single stripe direction.[8–10] Through investigations of the anisotropic optical response, supported by electron and x-ray diffraction measurements, it was concluded that the lone e_g electron orbitals of the Mn^{3+} ions order into stripes along the *a* axis below T_{OO1}, at 370 K (Fig. 2). As the system is cooled below T_{OO2}, at 300 K, these orbital stripes reorientate such that the stripes now run along the *b* axis. Although there is a small structural change both at T_{OO1} and T_{OO2}, the system remains orthorhombic throughout. Recently the rotation of the orbital stripes in $Pr(Sr,Ca)_2Mn_2O_7$ has been initiated through the application of uniaxial stress.[11]

Below the onset of orbital order (T_{OO1}), the space group is more properly described as *Pbnm*, followed by a further transition to *Am2m* at T_{OO2}. This takes into account the orbital order (and associated displacement of the Mn ions), and doubles the unit cell in the *a* and *b* axes, respectively. For clarity, however, we index the structural and orbital reflections for all phases in the *Amam* space group.

II. EXPERIMENTAL DETAILS

Samples of $Pr(Sr_{0.1}Ca_{0.9})_2Mn_2O_7$ were grown at the University of Oxford by the floating zone technique.[12,13] Small high quality samples were selected and prealigned with a

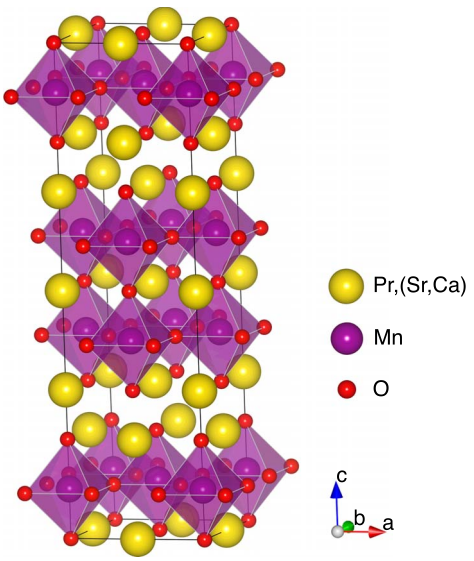

FIG. 1. (Color online) The crystal structure of $Pr(Sr_{0.1}Ca_{0.9})_2Mn_2O_7$. The Mn-O octahedra are shown by purple/gray polyhedra, with the black lines showing the extent of the crystallographic unit cell.

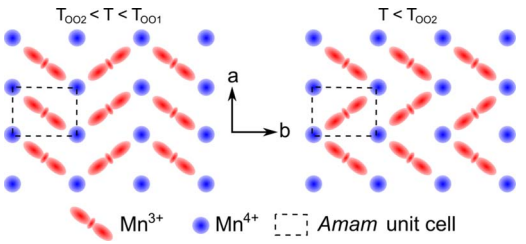

FIG. 2. (Color online) Schematic of the orbital stripes running along the *a* axis below T_{OO1}, and along the *b* axis below T_{OO2}. Note that the structure is orthorhombic above T_{OO1}, facilitating preferential stripe directions.

rotating anode x-ray source. Two such samples, aligned with the a/b-axis surface normal, were polished to a mirrorlike surface with 0.25 μm diamond suspension. Prior to the soft x-ray diffraction experiment these samples were studied with nonresonant (9.26 keV) high-resolution x-ray diffraction at BM28, ESRF. This showed both samples to be twinned, through a 90° rotation, with the reflections from *a*-axis and *b*-axis surface-normal domains approximately equal in intensity. Raster scanning the samples did not preferentially select either domain, suggesting that the domains were much smaller than the incident x-ray beam (100×300 μm^2). Despite this twinning, x-ray scattering has sufficient angular resolution to resolve, and therefore separate, the reflections from *a* and *b* directions. The sample giving the cleanest diffraction signal was then mounted in the in-vacuum six circle x-ray diffractometer on beamline ID08, ESRF. Diffraction measurements were undertaken using a horizontally (σ) polarized x-ray beam, provided by a single APPLE II undulator with an energy resolution in the region of the Mn *L* edges of 0.3 eV.

III. RESULTS AND DISCUSSION

A diffraction signal at the $(\frac{1}{2},0,0)$ orbital order reflection was found at room temperature at 652 eV (Fig. 3). Further slight warming to $T \approx 315$ K caused this peak to split, suggesting the coexistence of the $(\frac{1}{2},0,0)$ and $(0,\frac{1}{2},0)$ orbital reflections (albeit observed in different domains). After further warming to 330 K, only the $(0,\frac{1}{2},0)$ reflection remained.

The anisotropy of the scattering process from the orbital reflection was measured through rotation of the sample around the scattering vector. This measurement was taken on the I06 beamline at Diamond Light Source, using the two-circle in-vacuum diffractometer from Daresbury Laboratory. The measurement was made possible through the addition of a piezorotator providing a ϕ rotation. Figure 4 shows the azimuthal dependence of the intensity of the $(\frac{1}{2},0,0)$ and $(0,\frac{1}{2},0)$ reflections measured with horizontally (σ) polarized x rays at 140 and 327 K, respectively. The data are shown with the expected $\sin^2 \phi$ dependence calculated for each of these orbital structures. Periodic measurements of the intensity of the reflection were taken with vertically (π) polarized x rays, showing an identical azimuthal dependence as expected.

Figure 5 shows the variation in the intensity of the high-temperature $(0,\frac{1}{2},0)$ and low-temperature $(\frac{1}{2},0,0)$ reflections as a function of temperature. It is immediately obvious from the relative intensity of the reflections that the high-temperature orbital order is significantly weaker than the low-temperature phase. The inset of Fig. 5 shows a $\vec{Q}$ scan through the twinned (800)/(080) reflection as measured with hard (9.26 keV) x rays. The reflections from the two sets of domains were of relatively equal intensity; therefore the intensity of the $(0,\frac{1}{2},0)$ relative to the intensity of the $(\frac{1}{2},0,0)$ is a real measure of the orbital stripes in each phase, and not a result of an inequality in the domain sizes. No significant change in intensity was observed through scanning across the sample in either of the Bragg peaks using hard x rays or at either reflection observed at the Mn *L* edges. It is also noted that the low-temperature $(\frac{1}{2},0,0)$ orbital order signal is not affected by the antiferromagnetic order, showing no change in intensity at T_N.

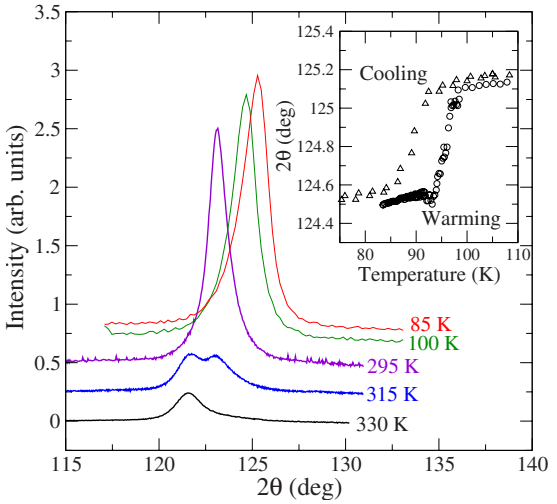

FIG. 3. (Color online) θ-2θ scans showing the diffraction signals in the different orbital phases. All scans were measured at 652 eV. The inset shows the change in position of the reflection through the low-temperature transition (T_S). The change in position of the reflection between 295 and 100 K is due to thermal contraction, and reflects a gradual change in lattice parameter rather than the abrupt change observed at 90 K.

The appearance of the $(\frac{1}{2},0,0)$ reflection at T_{OO2} occurs near the maximum intensity of the $(0,\frac{1}{2},0)$, suggesting that through cooling the formation of the orbital order stripes

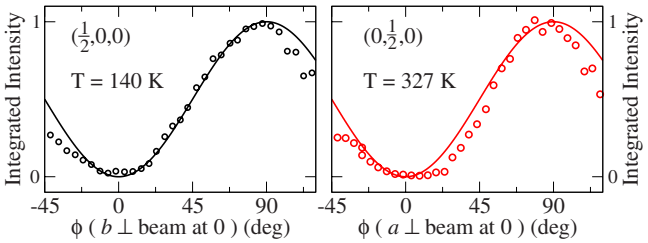

FIG. 4. (Color online) Anisotropy of the $(\frac{1}{2},0,0)$ and $(0,\frac{1}{2},0)$ orbital order reflections, measured by rotating the sample around the scattering vector. The solid line shows the calculated azimuthal dependence. Fitting errors of the peak intensity are within the symbol size.

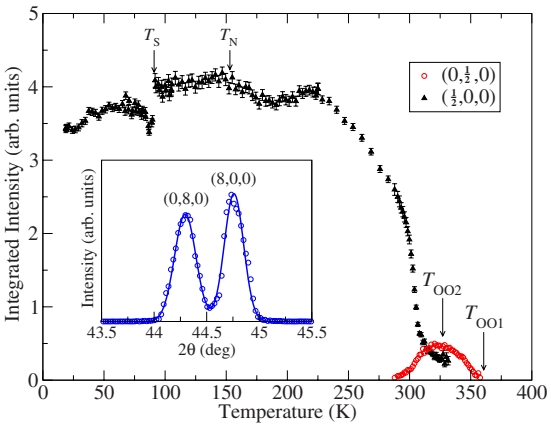

FIG. 5. (Color online) Temperature dependence of the orbital order reflections measured while cooling. The $(0,\frac{1}{2},0)$ reflection appears at T_{OO1}, with the $(\frac{1}{2},0,0)$ reflection forming at T_{OO2}. A further transition is observed at T_S. The inset shows the (800) and (080) reflections in the twinned sample measured at 9.26 keV at room temperature (solid line shows Gaussian fits).

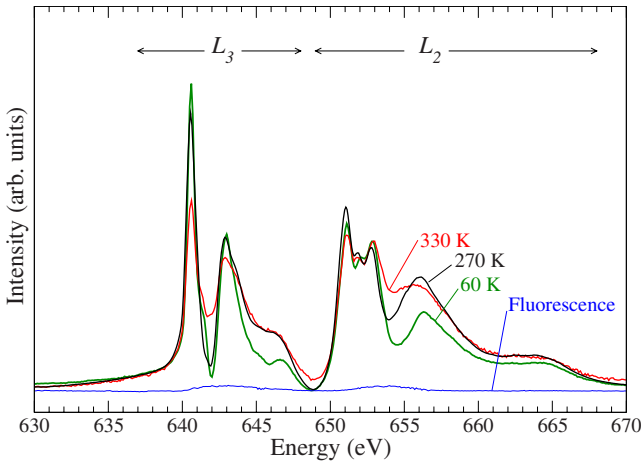

FIG. 6. (Color online) Energy scans at fixed wave vector from the orbital signal in different phases. The spectrum at 330 K is of the $(0,\frac{1}{2},0)$ reflection while the spectra at 270 and 60 K are of the $(\frac{1}{2},0,0)$ reflection. The energy spectra are all normalized at the main L_2 resonance, with the fluorescence (measured away from the reflection) on the same scale as the lowest intensity resonance at 330 K.

along the *b* axis destroys orbital stripes along the *a* axis. The simultaneous observation of both orbital reflections can be explained by a multidomain sample, where the orbital order rotates in some domains prior to others. Therefore by cooling through T_{OO2} the orbital order in each domain is rotated from stripes along the *a* axis to stripes orientated along the *b* axis, with this stripe reorientation occurring over approximately 30 K.

The formation of multiple orbital order domains in a single crystal is not unusual. In the tetragonal bilayer manganite series $La_{2-2x}Sr_{1+2x}Mn_2O_7$, reflections are observed both at $(\frac{1}{4},\frac{1}{4},0)$ and $(-\frac{1}{4},\frac{1}{4},0)$ ($I4/mmm$ symmetry), where orbital stripes occur in the $[\bar{1}10]$ and $[110]$ directions in different domains.[14,15] The difference is that the tetragonal system has no preferential direction for the orbitals to exist and as such are observed equally in both orbital domain directions at all temperatures below the orbital order transition. A similar occupation of multiple domains is observed in the monolayered[16] and cubic manganites. Chen and co-workers[17,18] used dark field imaging to demonstrate the presence of charge order domains (concomitant with orbital ordering) in $La_{1-x}Sr_xMnO_3$, with sizes of the order 100 nm.

The orbital reflections display complex energy spectra at the Mn *L* edges (Fig. 6) very similar to that observed in the tetragonal $LaSr_2Mn_2O_7$.[19] There are subtle differences between the energy spectra of the $(0,\frac{1}{2},0)$ and $(\frac{1}{2},0,0)$ reflections, in particular the pre-edge spike is more prominent in the $(\frac{1}{2},0,0)$ at 270 K, and the high energy features after the main L_2 edge are broader in energy in the $(0,\frac{1}{2},0)$ at 330 K. However, the energy spectra are generally similar, leading to the conclusion that the occupied orbital type is the same in both phases, existing in the $d_{3x^2-r^2}/d_{3y^2-r^2}$ (Ref. 10) above and below the transition.

A comparison of the energy spectra to the spectrum and calculations of the orbital reflection in $LaSr_2Mn_2O_7$ (Refs. 19 and 20) suggests that this system has a small but finite Jahn-Teller distortion. The relative sizes of the L_2 and L_3 edges are similar to those in $LaSr_2Mn_2O_7$. This ratio has been shown through ligand-field calculations to be sensitive to Jahn-Teller distortions,[21] where the tetragonal Jahn-Teller field parameter X^{220} was determined to be in the interval of 0.1–0.6 eV.[20] Cluster model calculations have shown that this ratio is also dependent on the spin correlation but agree with a small Jahn-Teller distortion.[22]

Within the low-temperature orbital phase, a further transition, T_S, was observed at 92 K, where there is a jump in the position of the orbital reflection (Fig. 3) accompanied by a small decrease in intensity (Fig. 5). This is briefly mentioned by Tokunaga *et al.*[8] and was attributed to a structural transition from orthorhombic to monoclinic. We investigated this transition further, using high energy (100 keV) x-ray diffraction at BW5, HASYLAB.[23] The positions of the (4,0,0), (0,4,0), and (0,0,16) Bragg reflections were measured on warming through the transition (Fig. 7). This shows a change in all three lattice parameters; however, we were insensitive to any small deviation of α from 90°. The observed increase in the 2θ value of the $(\frac{1}{2},0,0)$ (inset of Fig. 3) corresponds to a reduction in the *a* lattice parameter. This shows that this transition does not correspond to further change in the direction of the orbital stripes. The structural transition, T_S, shows thermal hysteresis, observed by the wave vector of the orbital reflection at T_S.

Figure 6 shows some differences between the spectrum at T=60 K and T=270 K. However, the spectra above and below T_S are virtually identical (Fig. 8), showing that the structural transition is not accompanied by any significant change in the orbital order. Rather, the change in the spectrum between 60 and 270 K is a gradual change that occurs as the sample is cooled. Although the structural transition reduces the orthorhombicity below T_S, we did not observe any sign of the reappearance of the $(0,\frac{1}{2},0)$ reflection. Therefore the orthorhombic strain remains sufficient to maintain the orbital order along the *a* axis below T_S.

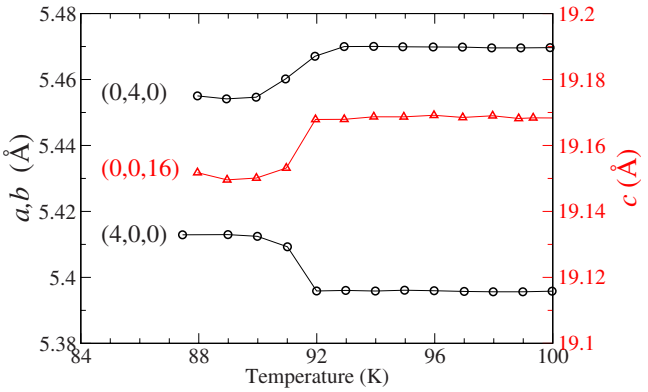

FIG. 7. (Color online) The lattice parameters of $Pr(Sr_{0.1}Ca_{0.9})_2Mn_2O_7$ measured though the positions of Bragg reflections in each direction. Measurements were taken using 100 keV x rays at beamline BW5, HASYLAB. The solid lines are guides to the eye.

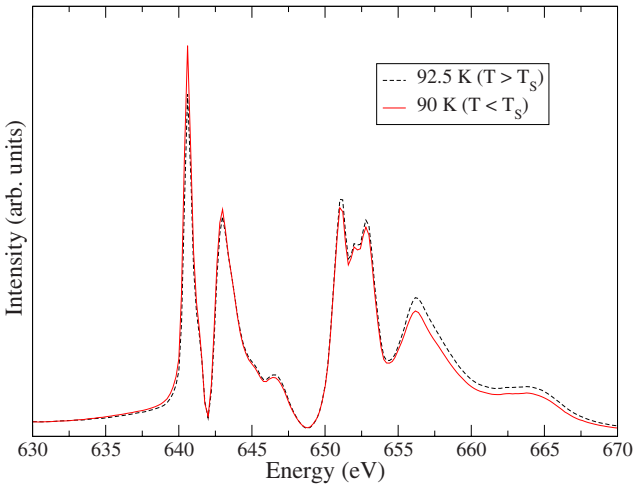

FIG. 8. (Color online) Energy scans at fixed wave vector from the orbital signal on either side of T_S through cooling the sample, showing no spectral change that would be indicative of an orbital occupancy change.

Constraining the formation of long-range-order parameters by the crystal lattice is not unique to $Pr(Sr_{0.1}Ca_{0.9})_2Mn_2O_7$. The monolayer nickelate $Pr_{2-x}Sr_xNiO_4$ has a tetragonal to orthorhombic transition well above the charge order transition restricting the formation of the charge stripes to parallel to the *a* axis.[24] Unlike the bilayer manganite studied here, there is no charge stripe reorientation. In the $La_{2-2x}Sr_{1+2x}Mn_2O_7$ series, charge and orbital orderings are observed where $x > 0.475$, in addition to low-temperature antiferromagnetism. Tokunaga *et al.*[10] studied the effect of varying the Sr,Ca doping in $Pr_{2-2x}(Sr_{1-y},Ca_y)_{1+2x}Mn_2O_7$ and found that the orbital rotation transition was present throughout the antiferromagnetic phase where $y \geq 0.4$. A change in Sr,Ca does not alter the hole concentration, and therefore the charge order in the system, which remains "half doped." It is unknown how strongly the orbital rotation is coupled to this charge order pattern, and how a change in the charge order, initiated through a change in the Pr (x) doping will effect the orbital rotation.

IV. CONCLUSION

In summary, we have directly observed the rotation of the orbital stripes in $Pr(Sr_{0.1}Ca_{0.9})_2Mn_2O_7$ through resonant soft x-ray diffraction and shown that the transition occurs gradually over a 30 K range in temperature. There is little significant change in the orbital resonant spectra suggesting that the orbital type and crystal field around the Mn^{3+} remains the same. We have observed structural changes taking place at $T = T_S$ but we do not observe any change in the occupation of the 3*d* orbitals at this transition. There is also no change in the orbital signal with the appearance of antiferromagnetic order at T_N.

ACKNOWLEDGMENTS

The authors would like to acknowledge the European Synchrotron Radiation Facility for the provision of synchrotron radiation at beamlines ID08 and BM28. Beamline BM28 is an EPSRC-GB-funded beamline at the ESRF, directed by M. J. Cooper and C. Lucas. We are grateful to the BM28 beamline team of P. Thompson, S. D. Brown, L. Bouchenoire, P. Normile, and D. F. Paul for their invaluable assistance, and to S. Beaufoy and J. Kervin for additional support. In addition we acknowledge Diamond Light Source for provision of synchrotron radiation, at beamline I06, and HASYLAB for synchrotron radiation at BW5. We thank M. D. Roper and A. Potenza for experimental support. T.A.W.B., S.R.B., R.D.J., and P.D.H. wish to thank EPSRC-GB and STFC for support.

*p.d.hatton@dur.ac.uk

[1] J. B. Goodenough, Phys. Rev. **100**, 564 (1955).
[2] Y. Murakami, H. Kawada, H. Kawata, M. Tanaka, T. Arima, Y. Moritomo, and Y. Tokura, Phys. Rev. Lett. **80**, 1932 (1998).
[3] B. J. Sternlieb, J. P. Hill, U. C. Wildgruber, G. M. Luke, B. Nachumi, Y. Moritomo, and Y. Tokura, Phys. Rev. Lett. **76**, 2169 (1996).
[4] C. D. Ling, J. E. Millburn, J. F. Mitchell, D. N. Argyriou, J. Linton, and H. N. Bordallo, Phys. Rev. B **62**, 15096 (2000).
[5] Y. Tokura, Phys. Today **56** (7), 50 (2003).
[6] Y. Konishi, Z. Fang, M. Izumi, T. Manako, M. Kasai, H. Kuwahara, M. Kawasaki, K. Terakura, and Y. Tokura, J. Phys. Soc. Jpn. **68**, 3790 (1999).
[7] L. Sudheendra, V. Moshnyaga, E. D. Mishina, B. Damaschke, T. Rasing, and K. Samwer, Phys. Rev. B **75**, 172407 (2007).
[8] Y. Tokunaga, T. Lottermoser, Y. Lee, R. Kumai, M. Uchida, T. Arima, and Y. Tokura, Nature Mater. **5**, 937 (2006).
[9] Y. S. Lee, Y. Tokunaga, T. Arima, and Y. Tokura, Phys. Rev. B

75, 174406 (2007).
[10] Y. Tokunaga, T. J. Sato, M. Uchida, R. Kumai, Y. Matsui, T. Arima, and Y. Tokura, Phys. Rev. B **77**, 064428 (2008).
[11] Y. Tokunaga, R. Kumai, N. Takeshita, Y. Kaneko, J. P. He, T. Arima, and Y. Tokura, Phys. Rev. B **78**, 155105 (2008).
[12] D. Prabhakaran and A. T. Boothroyd, J. Mater. Sci.: Mater. Electron. **14**, 587 (2003).
[13] D. Prabhakaran and A. T. Boothroyd, in *Frontiers in Magnetic Materials*, edited by A. Narlikar (Spinger-Verlag, Berlin, 2005), pp. 97–115.
[14] S. B. Wilkins, P. D. Spencer, T. A. W. Beale, P. D. Hatton, M. v. Zimmermann, S. D. Brown, D. Prabhakaran, and A. T. Boothroyd, Phys. Rev. B **67**, 205110 (2003).
[15] T. A. W. Beale, P. D. Spencer, P. D. Hatton, S. B. Wilkins, M. v. Zimmermann, S. D. Brown, D. Prabhakaran, and A. T. Boothroyd, Phys. Rev. B **72**, 064432 (2005).
[16] X. Yu *et al.*, Phys. Rev. B **75**, 174441 (2007).
[17] C. H. Chen, S.-W. Cheong, and H. Y. Hwang, J. Appl. Phys. **81**, 4326 (1997).
[18] C. H. Chen and S.-W. Cheong, Phys. Rev. Lett. **76**, 4042 (1996).
[19] S. B. Wilkins, N. Stojic, T. A. W. Beale, N. Binggeli, P. D. Hatton, P. Bencok, S. Stanescu, J. F. Mitchell, P. Abbamonte, and M. Altarelli, J. Phys.: Condens. Matter **18**, L323 (2006).
[20] S. B. Wilkins, N. Stojic, T. A. W. Beale, N. Binggeli, C. W. M. Castleton, P. Bencok, D. Prabhakaran, A. T. Boothroyd, P. D. Hatton, and M. Altarelli, Phys. Rev. B **71**, 245102 (2005).
[21] C. W. M. Castleton and M. Altarelli, Phys. Rev. B **62**, 1033 (2000).
[22] A. Mirone, S. S. Dhesi, and G. van der Laan, Eur. Phys. J. B **53**, 23 (2006).
[23] R. Bouchard *et al.*, J. Synchrotron Radiat. **5**, 90 (1998).
[24] M. Hücker *et al.*, Phys. Rev. B **74**, 085112 (2006).